Journal of the Serbian Chemical Society
JSCS-info@shd.org.rs • www.shd.org.rs/JSCS
J. Serb. Chem. Soc. 79 (9) 1155–1167 (2014)
JSCS–4654
UDC 546.723–31+546.26–162+
541.182.41:543.424.2:539.12
Original scientific paper

Ex situ integration of iron oxide nanoparticles onto exfoliated expanded graphite flakes in aqueous suspension

NATAŠA JOVIĆ[1]*, MARIA P. CALATAYUD[2], BEATRIZ SANZ[2], AMELIA MONTONE[3] and GERARDO F. GOYA[2]

[1]*Vinča Institute of Nuclear Sciences (020), University of Belgrade, P. O. Box 522, 11000 Belgrade, Serbia,* [2]*Aragón Institute of Nanoscience and Department of the Physics of Condensed Matter, University of Zaragoza, Zaragoza, Spain and* [3]*ENEA, Technical Unit Materials Technology, Research Centre of Casaccia, Via Anguillarese 301, 00123 Rome, Italy*

(Received 21 November 2013, revised 3 March, accepted 10 March 2014)

Abstract: Hybrid structures composed of exfoliated expanded graphite (EG) and iron oxide nanocrystals were produced by an *ex situ* process. The iron oxide nanoparticles coated with *meso*-2,3-dimercaptosuccinic acid (DMSA), or poly(acrylic acid) (PAA) were integrated onto the exfoliated EG flakes by mixing their aqueous suspensions at room temperature under the support of 1-ethyl-3-(3-dimethylaminopropyl)carbodiimide (EDC) and *N*-hydroxysuccinnimide (NHS). EG flakes both naked and functionalized with branched polyethylenimine (PEI) were employed. Complete integration of the two constituents was achieved and stability was maintained for more than 12 months. No preferential spatial distribution of anchoring sites for attachment of iron oxide nanoparticles was observed, regardless of whether the EG flakes were used naked or functionalized with PEI molecules. The structural and physicochemical characteristics of the exfoliated expanded graphite and its hybrid nanostructures were investigated by SEM, TEM, FTIR and Raman techniques.

Keywords: expanded graphite; iron oxide nanoparticles; nanocomposites; TEM; Raman spectroscopy.

INTRODUCTION

Due to its outstanding properties, graphene has been widely investigated. Recently, decoration of graphene platelets with different nanoparticles (quantum dots,[1] and magnetic[2] or noble metal nanoparticles[3–5]) has attracted great attention. Such graphene-based hybrid structures combine the properties of both constituents. Depending on a kind of employed nanoparticles, multifunctional hybrids can express magnetic, optically active, conducting, catalytic and electrochemically active properties, thereby simultaneously keeping the good characteris-

* Corresponding author. E-mail: natasaj@vinca.rs
doi: 10.2298/JSC131121019J

tics of graphene sheets, such as their stiffness, electrical conductivity and optical transparency. For example, graphene platelets decorated with transition metal or metal oxide nanoparticles were shown to be good candidates for the anode material in lithium-ion batteries,[2,6] or as effective adsorbents for the removal of organic molecules and heavy metal ions from waste water.[7–9] The properties of such hybrid structures are additionally dependent on the thickness of graphene platelets[10] (mono- or few-layer graphene), the structural defects inside the basal graphene plane, and/or the number of oxygen-containing functional groups on the surface.[11,12] Another important factor in defining the performances of hybrids could be related to the interfacial adhesion between the anchoring entities and the graphene support.[6]

The production of graphene platelets as substrates for hybrid structures is usually based on two different methods. The most common method to produce graphene platelets is the reduction of graphite oxide (GO) prepared from graphite according to the Hummers method.[13] However, this process involves the use of strong and harmful reducing reactants, such as hydrazine. Simultaneously, the restacking of graphene sheets usually results in: *i*) a corrugated-sheet structure with damages in the basal plane and *ii*) a surface enriched with oxygen residues. Another method to produce graphene platelets is based on the exfoliation of graphite by means of ultrasonic treatment.[14–16]

A hybrid structure with a graphene-based material as support matrix can be produced by different synthesis procedures, such as thermal decomposition of metal salts in the presence of graphene or graphene oxide sheets,[17–19] hydrothermal/solvothermal methods[20,21] or the simple mixing of solutions.[22] Methods based on the *in situ* approach (the synthesis of nanoparticles occurs in the presence of graphene or graphene oxide sheets) are commonly in use. Only a few studies followed an *ex situ* approach in which previously synthesized and functionalized nanoparticles were used to anchor the graphene sheets.[8,22] An overview of the literature data is presented in Table I, with emphases on the synthesis method, type of carbon-based matrix as support for the nanoparticles, type of bonding between constituents and possible application of graphene-based hybrid structures. Graphene-based hybrids can further be used as a filler in various polymer matrices,[23,24] for the production of thin films[1] or as colloids.[25]

In the present work, an *ex situ* process was used to decorate exfoliated expanded graphite (EG) sheets with *meso*-2,3-dimercaptosuccinic acid (DMSA)- or poly(acrylic acid) (PAA)-coated iron oxide nanoparticles (IONs). The aqueous suspensions of the two constituents were mixed at room temperature. This is one of the rare attempts where exfoliated expanded graphite,[27] obtained by reduction of graphene oxide, was used as the support instead of graphene sheets. The starting material was commercially available expanded graphite that was subjected to sonication in ethanol. The graphite flakes obtained in such a way were used

naked or grafted with PEI molecules and then were decorated with DMSA- or PAA-coated IONs in the presence of 1-ethyl-3-(3-dimethylaminopropyl)carbodiimide (EDC) and *N*-hydroxysuccinnimide (NHS). The morphology and structural properties of the exfoliated expanded graphite sheets and its hybrid structures with IONs were studied by SEM, TEM, FTIR and Raman techniques.

TABLE I. Iron oxide/carbon-based hybrid structures: methods of synthesis, types of support matrix/iron oxide nanoparticles, types of bonding, and potential applications of the hybrids; rGO – reduced graphene oxide

Method of synthesis	Graphene-based support/IONs	Type of bonding	Potential application
	In situ		
Co-precipitation of iron salts in water	rGO[a]/Fe_3O_4	–	Electrochemical detection of chromium[17]
Thermal decomposition of iron precursor in organic solvents	Graphene or rGO/Fe_3O_4	–	Wave filters; superconductors[10,18]
Hydrothermal method	Graphene/Fe_3O_4	Direct bonding (without molecular linkers)	In polymer matrix for optical devices; bioimaging[20]
Solvothermal reaction	Graphene/Fe_3O_4 microspheres	–	Loading of doxorubicin hydrochloride[21]
Direct pyrolysis of $Fe(NO_3)_3{\cdot}9H_2O$	Graphene/Fe_3O_4	*Via* Fe–O–C bond	In Li-ion batteries[6]
	Ex situ		
Ultrasonication	GO/Fe_3O_4	Covalent bonding/ assisted by EDC/NHS	For removing cationic dyes (Methylene Blue; Neutral Red)[8]
Mixing of aqueous solutions	PEI-grafted rGO/Fe_3O_4	Covalent bonding/ assisted by EDC/NHS	For removal of antibiotics or aromatic anticancer drugs[22]
Mixing of aqueous solutions	Graphene/Fe_3O_4	Covalent bonding assisted by EDC	For drug delivery (loading and release of 5-fluorouracil)[26]

EXPERIMENTAL

Materials

Commercial, highly expanded graphite (supplied by the Carbone Lorraine Group, France), iron(III) acetylacetonate ($Fe(acac)_3$, Aldrich, ≥97 %; IUPAC name: tris(acetylacetonato)iron(III)), iron(II) sulfate heptahydrate ($FeSO_4{\cdot}7H_2O$), oleic acid (90 % pure; IUPAC name: (9*Z*)-octadec-9-enoic acid), oleylamine (70 % pure; IUPAC name: (*Z*)-octa-9--decenylamine), 1,2-dodecandiol (90 % pure), 1-octadecene, hexane, toluene, *meso*-2,3-dimercaptosuccinic acid (DMSA, Sigma–Aldrich, ≈98 % pure; IUPAC name: 2,3-dimercaptobutanedioic acid), poly(acrylic acid) (PAA, 450 kDa), dimethyl sulfoxide (DMSO, Sigma––Aldrich, 99.9 % pure), triethylamine (PANREAC, 99.5 % pure), branched polyethylenimine (PEI, 25 kDa; IUPAC name: poly(iminoethylene)), 1-ethyl-3-(3-dimethyaminopropyl)carbo-

diimide (EDC; IUPAC name: 3-(ethyliminomethyleneamino)-*N*,*N*-dimethylpropan-1-amine)), *N*-hydroxysuccinnimide (NHS, Fluka, >97 %; IUPAC name: 1-hydroxy-2,5-pyrrolidine-dione), absolute ethanol, potassium nitrate (KNO_3) and sulfuric acid (H_2SO_4) were used as purchased.

Exfoliated expanded graphite (EG) flakes and its surface modified nanosheets (PEI–EG)

Commercial expanded graphite (EG, 0.2 g) in 50 ml of absolute ethanol was placed into an ultrasonic bath for 10 h. A certain amount of so obtained exfoliated EG flakes in absolute ethanol (concentration ≈4 mg mL^{-1}) were mixed with branched polyethylenimine (PEI, 25 kDa), previously dissolved in a mixture of milli-Q-water and dimethyl sulfoxide (DMSO) (1:4, *V*/*V*). The mass ratio of EG flake to PEI was 10:1. The mixture was agitated for two days in a rotatory mixer at room temperature. After mixing and rinsing with water, the surface-modified EG flakes were dispersed in milli-Q-water. The suspension of EG flakes was labeled as PEI–EG *aq*. (concentration ≈1 mg of EG per mL of H_2O). For the sake of comparison, a suspension of EG flakes in absolute ethanol was only rinsed several times with milli-Q-water and finally redispersed in water (naked EG flakes).

Synthesis and surface modification of iron oxide nanocrystals

Two types of iron oxide nanocrystals (IONs) were used to decorate the exfoliated expanded graphite flakes. One type of IONs was produced by thermal decomposition of iron(III) acetylacetonate salt in the presence of oleic acid and oleylamine in an organic solvent.[28] The second type of IONs was synthesized directly through an oxidative hydrolysis method.

Synthesis of iron oxide nanocrystals (IONs) by the thermal decomposition method and its surface modification with DMSA. The iron oxide nanocrystals were synthesized by the well--studied thermal decomposition method, starting from iron(III) acetylacetonate ($Fe(acac)_3$).[28] In brief, 2.825 g of $Fe(acac)_3$, 12.554 g of oleic acid, 15.286 g of oleylamine, and 8.992 g of 1,2-dedecandiol (mole ratio of 1:5:5:5) were added into in a three neck flask, previously filled with 80 mL of 1-octadecene. The solution was mechanically stirred at room temperature for 30 min under a nitrogen flow. Then, the mixture was heated to 200 °C, kept at that temperature for 2 h, further heated up to 290 °C under reflux conditions, aged at 290 °C for 30 min, and slowly cooled down to room temperature. The black precipitate was collected by a magnet and washed several times with ethanol and hexane. Finally, the precipitate was dissolved in toluene (the so-called stock solution). The concentration of IONs in the stock solution was determined by the UV–Vis spectroscopic approach[29] and was found to be ≈9.53 mg mL^{-1}.

In the next step, iron oxide nanocrystals (from the stock solution) were subjected to a surface exchange process in which the hydrophobic oleic acid molecules were replaced by the hydrophilic *meso*-2,3-dimercaptosuccinic acid (DMSA). The exchange process occurred in dimethyl sulfoxide (DMSO). IONs (10 mg), taken from the stock solution in toluene, were added into a DMSO solution of DMSA (20 mg mL^{-1}). Then, 50 µl of triethylamine was added, and the mixture was stirred at 60 °C for 17 h. The obtained black precipitate was collected by a pipette, transferred into microcentrifuge tubes, redispersed in absolute ethanol and centrifuged several times at 13000 rpm for 10 min in order to remove the free oleic acid molecules. Finally, the precipitated nanoparticles were redispersed in milli-Q-water. The obtained suspension was labeled as DMSA–ION.

Synthesis of PAA–ION nanocrystals by a modified oxidative hydrolysis method. The synthesis protocol used was based on the well-known oxidative hydrolysis method that consists of the precipitation of an iron salt ($FeSO_4$) in basic media (NaOH) with a mild oxidant. In a

typical synthesis, a mixture of 1.364 g of KNO_3 and 0.486 g of NaOH was dissolved in 135 mL of distilled water in a three-necked flask and bubbled with N_2. Then 15 mL of 0.01 M H_2SO_4 solution containing 0.3 g of $FeSO_4 \cdot 7H_2O$ and 0.30 g of poly(acrylic acid) (PAA, 450 kDa, previously bubbled with N_2 for 2 h) was added dropwise under constant stirring. When the precipitation was completed, nitrogen was allowed to pass through for another 5 min and the suspension with the black precipitate was held at 90 °C for 24 h under N_2. Afterwards, the solution was cooled to room temperature with an ice bath, and the solid was separated by a magnet, washed several times with distilled water and redispersed in milli-Q-water. The obtained suspension was labeled as PAA–ION. The concentration of iron oxide nanoparticles in the suspension was found to be ≈0.5 mg mL^{-1} (from the UV–Vis spectrum).

Preparation of iron oxide nanocrystals/expanded graphite hybrids

The four iron oxide/exfoliated expanded graphite hybrids were prepared by mixing of aqueous suspensions of exfoliated EG flakes with DMSA– and PAA–coated IONs. Exfoliated graphite flakes have been used naked (EG), or functionalized with branched polyethylenimine (PEI–EG *aq*.). The aqueous suspensions were mixed at room temperature in the presence of EDC and NHS. Details about production of the DMSA–ION/PEI–EG-2 nanohybrid structures are given below. The number at the end of sample's name represents the mass ratio between the loaded IONs and EG flakes in the sample.

Sample DMSA–ION/PEI–EG-2. 0.5 mg of graphite flakes functionalized with PEI molecules (PEI–EG *aq*.) was added into 1 mL of milli-Q-water, followed by addition of 5 mg of EDC and 5 mg of NHS. Then, 1 mg of iron oxide nanoparticles coated with DMSA and suspended in milli-Q-water (DMSA–ION), was added by dropwise into the mixture and stirred for two days at room temperature. The concentration of IONs in the solution was determined by UV–Vis spectroscopy.[29] The mixture was than collected, transferred into plastic tubes and washed in excess milli-Q-water three times (centrifuged at 4000 rpm for 10 min).

For the other three samples, EG flakes were decorated with PAA–coated IONs (PAA–ION) by the same procedure. In order to study possible influence of the PEI molecules on the attachment strength of PAA–IONs, naked EG flakes were used instead of PEI-grafted ones (sample PAA–ION/naked–EG-0.1). The mass amounts of all ingredients mixed, relative to EG, are given in Table II. The hybrids were labeled according to the type of IONs used and EG flakes, and their relative mass amounts.

Table II. The mass amount relative to exfoliated expanded graphite flakes (EG) of iron oxide nanoparticles (ION), 1-ethyl-3-(3-dimethyaminopropyl) carbodiimide (EDC), and *N*-hydroxy-succinnimide (NHS) used in preparation of the hybrid structures

Sample	ION	EDC	NHS
DMSA–ION/PEI–EG-2	2	10	10
PAA–ION/PEI–EG-0.5	0.5	10	10
PAA–ION/PEI–EG-0.1	0.1	1	1
PAA–ION/naked–EG-0.1	0.1	1	1

Characterization and measurements

The structural features of the expanded graphite (EG) flakes were investigated by X-ray diffraction (Bruker D8 Advance diffractometer, in the glaze angle (2°) incident geometry; λ = 1.5406 nm, I = 30 mA; V = 38 kV). Scanning electron microscopy (SEM, Cambridge, Stereoscan 250 Mk3) was used to observe the morphological features of EG and exfoliated

EG flakes. The hybrid structures built of naked or PEI-grafted EG flakes, and DMSA- or PAA-coated iron oxide nanoparticles were studied by transmission electron microscopy (TEM, FEI TECNAI T20, 200 kV), attenuated total reflectance infrared (ATR-FTIR, Bruker, Vertex 70) and Raman spectroscopy (Thermo Scientific DXR MicroRaman). The ATR-FTIR spectra were acquired in the 400–4000 cm^{-1} region with a resolution of 4 cm^{-1}, by accumulating 40 scans. The Raman spectra were collected in the spectral range 60–3100 cm^{-1} using a HeNe 532 nm gas laser with laser power 9.8 or 2 mW. The samples were previously casted onto a glass holder and dried at 40 °C for 3 h to eliminate water.

RESULTS AND DISCUSSION

The X–ray diffraction (XRD) pattern of pristine expanded graphite before sonication in ethanol revealed the presence of a diffraction peak at 26.5° which belongs to the (002) reflection of the hexagonal graphite structure (see inset in Fig. 1a). The average crystallite thickness along the (001) direction of the pristine expanded graphite, L_c, was estimated using the Scherrer Equation: $L_c = K\lambda/(\beta_{002}\cos\theta)$, and the integral width of (002) reflection, β_{002}, and it was found to be around 20 nm (K = 0.9). Bearing in mind that for ideal graphite, the interlayer distance along the c axis, d_{002}, is 0.335 nm, this means that the accordion-like pristine graphite (Fig. 1a and b) was built of bundles of expanded graphite sheets composed of approximately 60 graphene layers. SEM images of the exfoliated expanded graphite (EG) flakes obtained after sonication in absolute ethanol for 10 h (Fig. 1c and d) revealed that under ultrasonic treatment, thin and transparent nanosheets with high aspect ratio had been produced. The lateral dimensions of the EG flakes range from 2 to 20 μm. Based on the SEM micrographs, it could be

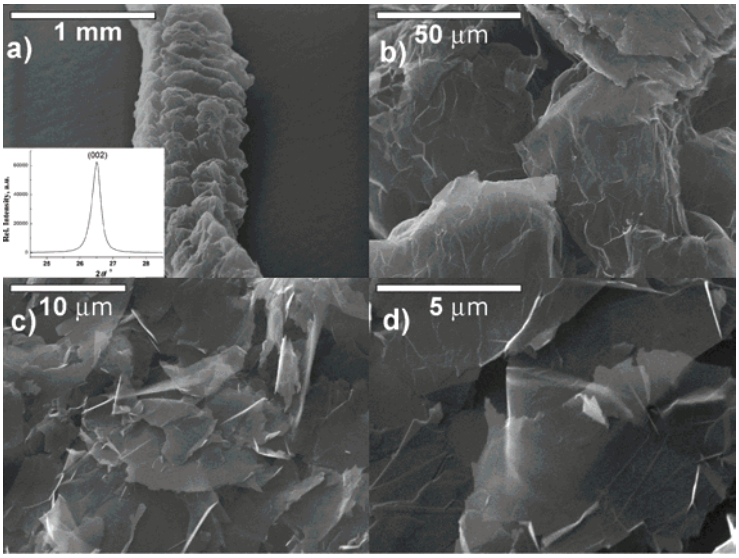

Fig. 1. SEM Images of: a) and b) expanded graphite (EG); c) and d) exfoliated EG. Inset: the XRD profile of (002) reflection of EG.

noticed that additional cleavage of EG flakes had occurred under ultrasonic irradiation, giving rise to foliation and the production of EG flakes thinner than those found in the pristine expanded graphite. This statement was additionally corroborated by Raman spectroscopy, as follows.

The Raman spectra of pristine and exfoliated EG flakes (after ultrasonic treatment) are shown in Fig. 2a. In the Raman spectrum of pristine EG flakes, a weak D band at ≈1360 cm^{-1}, a G band at ≈1585 cm^{-1} and an asymmetric 2D band were detected. The 2D band was deconvoluted into two Lorentzian peaks: the one at ≈2725 cm^{-1} with a full width at half maximum, FWHM of 38 cm^{-1}, and another at ≈2688 cm^{-1} with a FWHM of 59 cm^{-1} (Fig. 2b). A split 2D band that can be fitted by two peaks is characteristic of a 3–dimensional graphitic materials.[27,30] The low intensity of the D band indicated to the large lateral dimension of the EG sheets. Upon sonication in ethanol for 10 h, the intensity of the D–band (at ≈1350 cm^{-1}) increased, which could be assigned to the involvement of defects and disordering in the hexagonal graphitic layers upon ultrasound treatment. Simultaneously, the G–band at ≈1579 cm^{-1} became broader. The 2D--band of the exfoliated EG flakes was also fitted by two Lorentzian peaks with maxima at 2717 (FWHM = 38 cm^{-1}) and 2685 cm^{-1} (FWHM = 75 cm^{-1}, Fig.

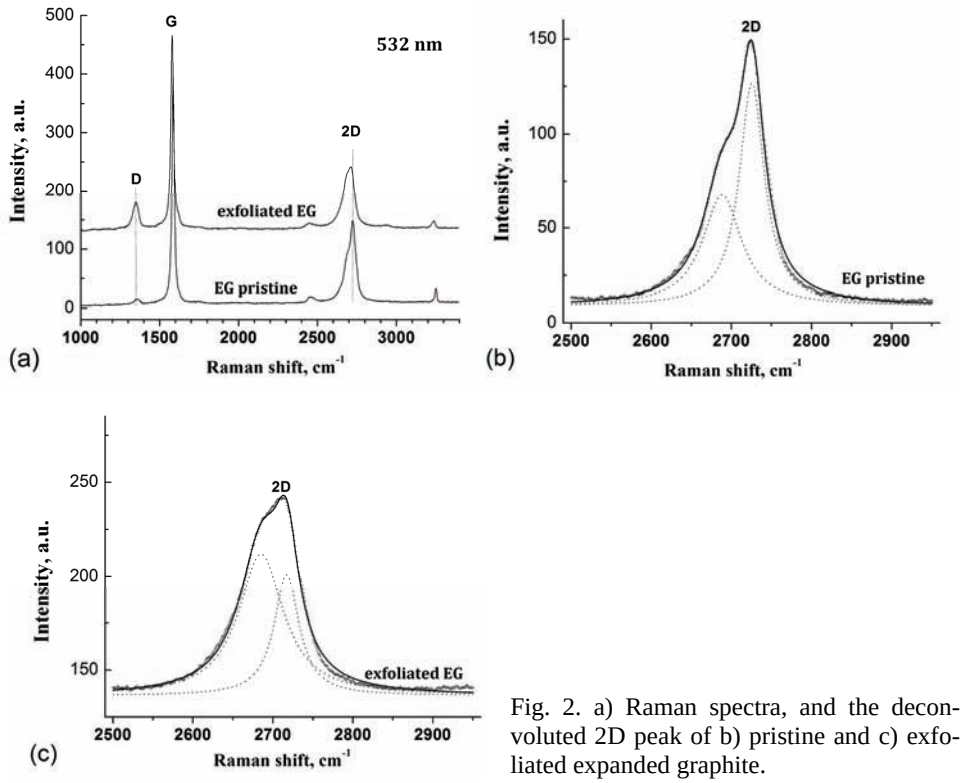

Fig. 2. a) Raman spectra, and the deconvoluted 2D peak of b) pristine and c) exfoliated expanded graphite.

2c). The relative intensities of these two Lorentzian components changed upon sonication, which indicated different degrees of stacking order along the *c* direction.[30]

The ATR-FTIR spectra of the naked and PEI–grafted EG flakes, and the PAA–ION/PEI–EG-0.5 hybrid showed very similar, almost featureless characteristics (Fig. 3). Such behavior is probably caused by the dark gray color of the exfoliated EG flakes. Closer inspection of these spectra (inset of Fig. 3) showed the presence of a weak transmittance peaks at 870 cm^{-1} in all three samples, which could be assigned to the asymmetric ring stretching.[31] An additional broad peak centered at *c.a.* ≈1100 cm^{-1} observed in the FTIR spectrum of the PEI--grafted EG flakes could be assign to the C–N stretching vibration peak for primary amines[32] (1130 cm^{-1}), and/or the presence of C–O groups (1060 cm^{-1}).[33] A transmittance band at *c.a.* ≈660 cm^{-1} in the FTIR spectrum of the PAA–Fe_3O_4/PEI–EG-0.5 hybrid could be attributed to Fe–O bonds. Due to nearly featureless nature of FTIR spectra, it is difficult to recognize the presence/absence of functional groups at the surface of the EG flakes. Nevertheless, the PEI-grafted EG flakes showed that better dispersion in water in comparison

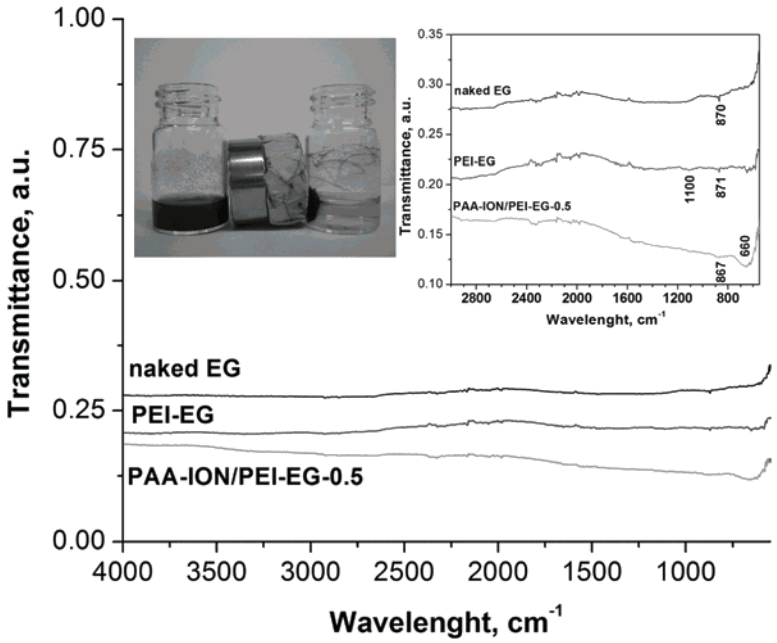

Fig. 3. ATR–FTIR spectra of exfoliated EG flakes (naked and PEI–grafted) and a selected hybrid, PAA–ION/PEI–EG-0.5. Inset (left): Response of water suspensions of pure exfoliated EG fakes and the response of the PAA–ION/PEI–EG-0.5 hybrid to the presence of a strong permanent magnet. Inset (right): Magnified ATR–FTIR spectra.

to the naked EG flakes. In addition, it was observed that if aqueous suspensions of both kinds of EG flakes were subjected to centrifugation under the same conditions, the PEI-grafted EG flakes precipitate while the naked EG flakes still float, which clearly indicates a difference in density of these two types of EG flakes. It is likely that the positively charged PEI molecules attached to the surface of the EG sheets produce surface charge changes, thus causing a weakening of hydrophobicity and an improvement in the stability of the dispersion of PEI--grafted EG flakes in water.

During the formation of hybrid structures between the PEI-grafted EG flakes and DMSA- and PAA-coated IONs, the amino groups ($–NH_2$) of the PEI molecules could react with the free carboxyl (–COOH) and thiol (–SH) groups of the DMSA molecules, as well as with the –COOH groups of the PAA molecules. The role of the EDC molecules is to activate the carboxylic groups for direct conjugation to primary amines and thus facilitate the attachment of iron oxide nanoparticles onto the EG flakes. Complete integration of IONs onto the exfoliated expanded graphite flakes in the PAA–ION/PEI–EG-0.5 hybrid was verified by its attraction to a strong permanent magnet (see inset of Fig. 3), while the naked EG flakes were not attracted. The microstructure of the DMSA–ION/PEI–EG-2

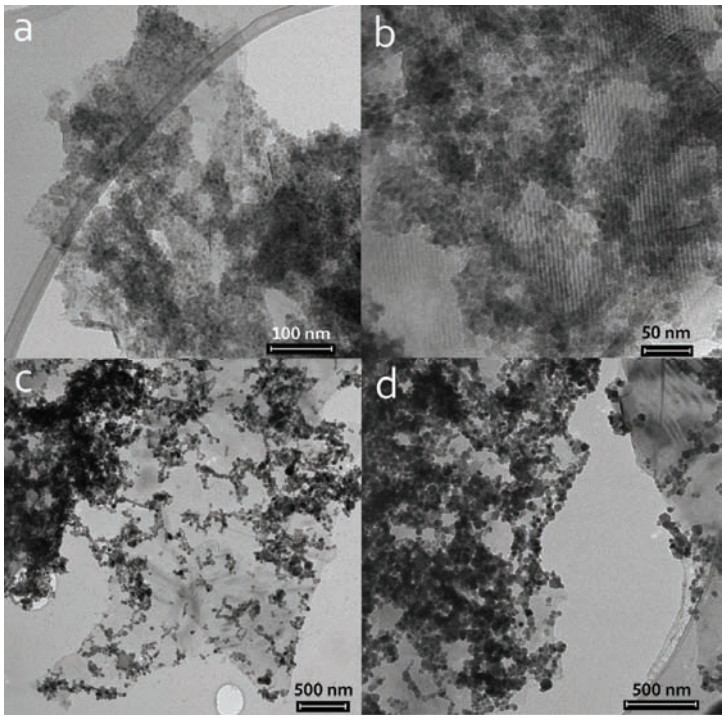

Fig. 4. TEM Images of a) and b) DMSA–ION/PEI–EG-2, and c) and d) PAA–ION/PEI–EG-0.5 hybrids.

and PAA–ION/PEI–EG-0.5 hybrids, shown in Fig. 4, indicate that the iron oxide nanoparticles are randomly distributed on the basal plane of the PEI-grafted EG flakes and they are agglomerated or form clusters of nanoparticles. Any preferential site for attachment of the IONs onto exfoliated EG sheets was not registered. On the contrary, Zhang *et al*., achieved a preferential periphery decoration of the graphene oxide sheets by magnetic nanoparticles caused by a difference in the spatial distribution of the oxygen-containing groups attached onto GO sheets (the carboxylic groups are located on the edge, while the epoxy and hydroxyl groups are usually located on the basal plane of GO sheets).[22]

To check if there were any influence of the PEI molecules on the assembly process of coated magnetic nanoparticles with EG flakes, two hybrids were introduced with the same nanoparticle loading (10 wt. % of PAA–IONs), using PEI--grafted and naked EG flakes as substrates (PAA–ION/PEI–EG-0.1 and PAA–ION/naked–EG-0.1 samples, respectively). In both cases, the integration of iron oxide nanoparticles with EG flakes was achieved. The TEM micrographs of

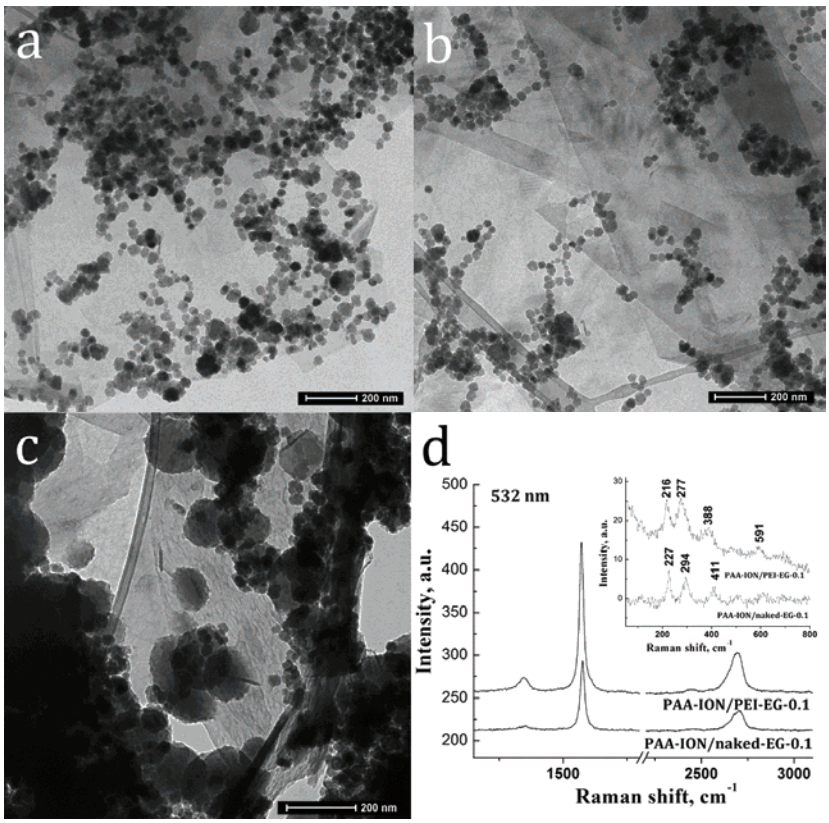

Fig. 5. TEM Micrographs of a) and b) PAA–ION/PEI–EG-0.1, c) PAA–ION/naked–EG-0.1 hybrids and d) the Raman spectra.

these two hybrids are shown in Fig. 5. Dark spots, observed only in the TEM micrograph of PAA–ION/naked–EG-0.1 hybrid, can be an indication of the presence of water droplets on a surface of the naked EG flakes. This could be explained by the difference in the macroscopic wetting behavior of water droplets on the naked and PEI-grafted EG sheets due to a difference in the binding energy (given by the Lennard–Jones potential) between a water monomer on one side and naked or PEI-grafted EG flakes on the other side.[34]

The Raman spectra of these two nanohybrids, PAA–ION/PEI–EG-0.1 and PAA–ION/naked–EG-0.1, are shown in Fig. 5c. In order to avoid degradation of PAA, the spectra were recorded with lower laser power. The intensity of the Raman bands characteristic for the exfoliated EG structure decreases. The Raman modes at 227, 294 and 411 cm^{-1} found in the spectrum of the PAA–ION/ /naked–EG-0.1 sample indisputably correspond to the hematite phase (inset of Fig. 5c). In the sample PAA–ION/PEI–EG-0.1, the characteristic Raman modes for hematite are shifted to 216, 277 and 388 cm^{-1}, respectively. The appearance of the α–Fe_2O_3 (instead of the expected magnetite) phase could have resulted from the laser treatment on the IONs during collection of the Raman spectrum.

As can be seen, the IONs are attached on the surface of the exfoliated EG flakes, either naked or PEI-grafted, without any preferential sites along the EG sheets for attachment of nanoparticles. This could be an indication that either the PEI molecules are not preferentially anchored along the border of the EG flakes, or it might also be that epoxy groups or some structural defects inside the honeycomb graphene lattice serve as anchoring sites.

CONCLUSIONS

In summary, successful decoration of exfoliated expanded graphite (EG) flakes with DMSA- or PAA-coated iron oxide nanoparticles was achieved by an *ex situ* process through the mixing of aqueous suspensions of two constituents at room temperature. The integration of the EG flakes and iron oxide nanoparticles was supported by EDC and NHS molecules. The bonds between the hybrid constituents were stable for more than 12 months. No preferential spatial distribution of anchoring sites for attachment of iron oxide nanoparticles was observed, regardless of whether the employed EG flakes were naked or functionalized with PEI molecules. This can indicate that other oxygen–containing functional groups (epoxy and/or hydroxyl) or structural defects inside graphene plane might serve as anchoring sites.

Acknowledgements. This work was supported by the Ministry of Education, Science and Technological Development of the Republic of Serbia through Project No. 45015. N. J. would like to thank the Ministry of Education, Science and Technological Development of the Republic of Serbia for a Postdoctoral fellowship at the Institute of Nanoscience of Aragon, University of Zaragoza, Spain (2010/2011). We thank Dr. Danica Bajuk-Bogdanović for performing the Raman measurements.

ИЗВОД

EX SITU УГРАЂИВАЊЕ НАНОЧЕСТИЦА ГВОЖЂЕ ОКСИДА НА ЛИСТИЋЕ ЕКСПАНДИРАНОГ ГРАФИТА У ВОДЕНОЈ СУСПЕНЗИЈИ

НАТАША ЈОВИЋ[1], MARIA P. CALATAYUD[2], BEATRIZ SANZ[2], AMELIA MONTONE[3] и GERARDO F. GOYA[2]

[1]*Институт за нуклеарне науке Винча (020), Универзитет у Београду, п.пр. 522, 11001 Београд,* [2]*Aragón Institute of Nanoscience and Department of Physics of Condesed Matter, University of Zaragoza, Zaragoza, Spain и* [3]*ENEA, Technical Unit Materials Technology, Research Centre of Casaccia, Via Anguillarese 301, 00123 Rome, Italy*

Хибридне наноструктуре изграђене од наночестица оксида гвожђа и листића експандираног графита добијене су *ex situ* поступком. Водене суспензије наночестица оксида гвожђа, претходно обложених молекулима мезо-2,3-димеркаптосукцинском киселином (DMSA), односно молекулима поли(акрилне киселине) (PAA), и листића експандираног графита мешане су на собној температури уз додатак 1-етил-3-(3-диметиламинопропил)карбодимида (EDC) и *N*-хирдоксисукцинимида (NHS). Коришћени су чисти и полиетиленимином (PEI) фукнционализовани листићи графита. Постигнуто је комплетно сједињавање две компоненете, а разградња хибридних структура није уочена ни након годину дана. Одсуство преферентне просторне расподеле места на графитним листићима за која се каче наночестице оксида гвожђа такође није уочена, без обзира на то да ли су коришћени чисти или функционализовани листићи графита. Структурна и физичко–хемијска својства листића експандираног графита и хибридних структура испитивана су применом скенирајуће и трансмисионе електронке микроскопије и инфрацрвене и Раманове спектроскопије.

(Примљено 21. новембра 2013, ревидирано 3. марта, прихваћено 10. марта 2014)

REFERENCES

1. X. Geng, L. Niu, Z. Xing, R. Song, G. Liu, M. Sun, G. Cheng, H. Zhong, Z. Liu, Z. Zhang, L. Sun, H. Xu, L. Lu, L. Liu, *Adv. Mater*. **22** (2010) 638
2. Z. S. Wu, W. Ren, L. Wen, L. Gao, J. Zhao, Z. Chen, G. Zhou, F. Li, H. M. Cheng, *ACS Nano* **4** (2010) 3187
3. B. S. Kong, J. Geng, H. T. Jung, *Chem. Comm*. (2009) 2174
4. M. Liu, H. Zhao, S. Chen, H. Yu, X. Quan, *ACS Nano* **6** (2012) 3142
5. H. Wu, J. Wang, X. Kang, C. Wang, D. Wang, J. Liu, I. A. Aksay, Y. Lin, *Talanta* **80** (2009) 403
6. J. Zhou, H. Song, L. Ma, X. Chen, *RSC Adv.* **1** (2011) 782
7. P. Bhunia, G. Kim, C. Baik, H. Lee, *Chem. Comm.* **48** (2012) 9888
8. F. He, J. Fan, D. Ma, L. Zhang, C. Leung, H. Laiwa Chan, *Carbon* **48** (2010) 3139
9. Y. W. Liu, M. X. Guan, L. Feng, S. L. Deng, J. F. Bao, S. Y. Xie, Z. Chen, R. B. Huang, L. S. Zheng, *Nanotechnology* **24** (2013) 025604
10. J. Zhu, Z. Luo, S. Wu, N. Haldoaarachchige, D. P. Young, S. Wei, Z. Guo, *J. Mater. Chem*. **22** (2012) 835
11. L. Ćirić, D. M. Djokić, J. Jaćimović, A. Sienkiewicz, A. Magrez, L. Forró, Ž. Šljivančanin, M. Lotya, J. N. Coleman, *Phys. Rev., B* **85** (2012) 205473
12. Q. Tang, Z. Zhou, Z. Chen, *Nanoscale* **5** (2013) 4541
13. W. S. Hummers Jr., R. E. Offeman, *J. Am. Chem. Soc*. **80** (1958) 1339
14. G. Chen, W. Weng, D. Wu, C. Wu, J. Lu, P. Wang, X. Chen, *Carbon* **42** (2004) 753
15. I. Zaman, H. C. Kuan, Q. Meng, A. Michelmore, N. Kawashima, T. Pitt, L. Zhang, S. Gouda, L. Luong, J. Ma, *Adv. Funct. Mater.* **22** (2012) 2735

16. J. Malig, C. Romero-Nieto, N. Jux, D. M. Guldi, *Adv. Mater*. **24** (2010) 800
17. A. Prakash, S. Chanda, D. Bahadur, *Carbon* **50** (2012) 4209
18. H. P. Cong, J. J. He, Y. Lu, S. H. Yu, *Small* **6** (2010) 169
19. D. W. P. Pang, F. W. Yuan, Y. C. Chang, G. A. Li, H. Y. Tuan, *Nanoscale* **4** (2012) 4562
20. L. Ren, S. Huang, W. Fan, T. Liu, *Appl. Surf. Sci*. **258** (2011) 1132
21. K. Zhou, Y. Zhu, X. Yang, C. Li, *New J. Chem*. **34** (2010) 2950
22. Y. Zhang, B. Chen, L. Zhang, J. Huang, F. Chen, Z. Yang, J. Yao, Z. Zhang, *Nanoscale* **3** (2011) 1446
23. T. T. Tung, J. F. Feller, T. Y. Kim, H. Kim, W. S. Yang, K. S. Suh, *J. Polym. Sci., A* **50** (2012) 927
24. X. Xia, Q. Hao, W. Lei, W. Wang, D. Sun, X. Wang, *J. Mater. Chem*. **22** (2012) 16844
25. S. Stankovich, R. D. Piner, X. Chen, N. Wu, S. T. Nguyen, R. S. Ruoff, *J. Mater. Chem.* **16** (2006) 155
26. X. Fan, G. Jiao, W. Zhao, P. Jin, X. Li, *Nanoscale* **5** (2013) 1143
27. G. Katsukis, J. Malig, C. Schulz-Drost, S. Leubner, N. Jux, D. M. Guldi, *ACS Nano* **6** (2012) 1915
28. S. Sun, H. Zeng, *J. Am. Chem. Soc*. **124** (2002) 8204
29. M. P. Calatayud, C. Riggio, V. Raffa, B. Sanz, T. E. Torres, M. R. Ibarra, C. Hoskins, A. Cuschieri, L. Wang, J. Pinkernelle, G. Keilhofff, G. F. Goya, *J. Mater. Chem., B* **1** (2013) 3607
30. M. A. Pimenta, G. Dresselhaus, M. S. Dresselhaus, L. G. Cançado, A. Jorio, R. Saito, *Phys. Chem. Chem. Phys*. **9** (2007) 1276
31. M. Lotya, Y. Hernandez, P. J. King, R. J. Smith, V. Nicolosi, L. S. Karlsson, F. M. Blighe, S. De, Z. Wang, I. T. McGovern, G. S. Duesberg, J. N. Coleman, *J. Am. Chem. Soc*. **131** (2009) 3611
32. Z. Qian, M. A. Khan, S. Mikkelsen, P. Chen, *Langmuir* **26** (2010) 2176
33. Y. Si, E. T. Samulski, *Nano Lett*. **8** (2008) 1679
34. T. Werder, J. H. Walther, R. L. Jaffe, T. Halicioglu, P. Koumoutsakos, *J. Phys. Chem*., *B* **107** (2003) 1345.